Toughened Polypropylene with Balanced Rigidity. IV. Morphology, Crystallization Behavior, and Thermal Properties

HONGJIE ZHANG, JINGWU WANG, SHAOKUI CAO, YONG WANG

Department of Materials Engineering, Zhengzhou University, Zhengzhou 450052, People's Republic of China

ABSTRACT: The morphology of toughened polypropylene with balanced rigidity (TRPP) was characterized by using transmission electron microscopy and polarizing light microscopy. The crystallization behavior and thermal properties were investigated by differential thermal analysis and thermogravimetric analysis. The PP component in the polymer blend was realized as the continuous phase and the elastomer component as the dispersed phase with a cellular structure (salami structure) containing some PP. The particles of the dispersed phase were small and regular. The cellular structure of the TRPPs resulted from the introduction of toughening master batches and was similar to the morphology of acrylonitrile-butadiene-styrene and high-impact polystyrene synthesized by graft copolymerization. By gradually cooling from the melt, crystallization of TRPPs was nucleated heterogeneously and the crystallization temperature was slightly higher than that of PP whereas the crystallite size was remarkably reduced. For the samples with different compositions, the number, shape, and size of the cellular dispersed particles and the crystallite size were different. Considering the toughening theories and our experimental data, it was concluded that the samples with more regular and small cellular dispersed particles generally had better mechanical properties and the remarkably reduced crystallite size of PP was favorable for toughness improvement. The melting point, thermal oxidation temperature, and thermal oxidation onset temperature of the TRPPs were all a little lower than those of PP and the processability remained good. © 2000 John Wiley & Sons, Inc. J Appl Polym Sci 79: 1351–1358, 2001

Key words: toughened polypropylene; balanced rigidity; morphology; crystallization behavior; thermal properties

INTRODUCTION

Blends of polyolefins with ethylene-propylene (EP) copolymer, butyl rubber, styrene-butadiene-styrene (SBS) elastomer, and so forth were extensively investigated with the aim of improving their mechanical properties.[1–5] A thorough understanding of the blend morphology is important, because of its great contribution to the properties of polymer blends.[6–8] The impact strength of incompatible polymer blends is closely related to the number, shape, and morphology of the dispersed phase particles.[9–13] These relationships are described in the literature. Zhang et al.[14–16] investigated a polypropylene/high density polyethylene/SBS (PP/HDPE/SBS) ternary blend system and found that complex HDPE/SBS particle configurations in packaged, network, or combined

forms were the particular morphological structures responsible for imparting high impact strength to the materials. Petrovic et al.[17] found that the notched Izod impact strength of PP/EP rubber (EPR) binary blends was enhanced by the addition of EPRs, particularly those containing PE. The contribution of PE was explained by a specific EPR/PE particle core–shell or interpenetrating morphology. D'Orazio et al.[18] compared the melt rheology, phase morphology, and properties of isotactic PP/EPR blends containing EPR copolymer synthesized by using a titanium-based catalyst (EPR_{Ti}) and a traditional vanadium-based catalyst (EPR_V), respectively. They ascribed the different behaviors of EPR_{Ti} and EPR_V as impact modifiers to both their different dispersion degree and microstructure.

In previous articles[19,20] we reported the preparation of toughening master batches (TMBs) in a low viscosity reaction system by using dynamic vulcanization techniques, starting with PP as the matrix resin and EP or SB elastomers as the toughening agent through polymer-bridge conjunction derived from a monomer containing a carbonyl group in the presence of a free-radical initiator. The chemical structure, morphology, melt flow rate, and melting point of the TMBs and the effect of various technical conditions were investigated. The mechanical properties of toughened PPs with balanced rigidity (TRPPs) produced with the above TMBs were also reported.[21]

The present article concentrates on the investigation of the morphology, crystallization behavior, and thermal properties of the TRPP blends made by blending TMB and PP resin.

EXPERIMENTAL

Materials

The TRPP was prepared by thermal mechanical blending of PP with a TMB as described in Zhang et al.[21] The materials used for preparation of the TMBs and TRPPs are given in the literature.[19,21] The compositions for samples used in this study are listed in Table I.

Phase Analysis

The molded TRPPs were trimmed into a cone shape and stained with osmium tetroxide (OsO_4) vapor to highlight the unsaturated diene phase. A Hitachi H-600 transmission electron microscope

Table I   Compositions of TRPPs

	M + N in TRPP (wt %)	TMB Used	M + N in TMB (wt %)	M/N (w/w) in TMB
PP	0	—	—	—
0G-0i	14	0i	32	80/20
4G-I-1	14	I-1	32	20/80
4G-I-2	14	I-2	32	40/60
4G-I-3	14	I-3	32	60/40
4G-I-4	14	I-4	32	80/20
4G-I-5	14	I-5	32	100/0
1G-I-4	8	I-4	32	80/20
2G-I-4	10	I-4	32	80/20
3G-I-4	12	I-4	32	80/20
4G-I-4	14	I-4	32	80/20
5G-I-4	16	I-4	32	80/20
4G-I-4	14	I-4	32	80/20
4G-II-4	14	II-4	38	80/20
4G-III-4	14	III-4	44	80/20
4G-IV-4	14	IV-4	50	80/20

M, ethylene-propylene elastomer; N, styrene-butadiene elastomer. In the TRPP the total weight of PP and elastomers is considered as 100 and the antioxidant is 0.05 wt % of the total resin. In the TMB the total weight of PP and elastomers is considered as 100, the bridging agent is 12 wt % of the total resin, and the initiator is 10 wt % of the bridging agent.

was used to observe microtomed slices of the stained TRPPs.

Crystalline Morphology Observation

An XP3C polarizing microscope (Guizhou Xintian Optical Precise Instrument Corporation) was used to observe the crystalline morphology of the TRPPs. Samples for polarizing microscopic study were prepared by heating the materials to 240 ± 2°C and maintaining the temperature for 3 min and then pressing for 10 s. After holding the samples at this temperature for another 5 min, the samples were cooled to 140 ± 1°C at a controlled cooling rate of 2°C/min, which was maintained for 30 min; then they were allowed to cool naturally to room temperature.

Crystallization Behavior and Thermal Properties Measurements

An LCT differential thermal analyzer (Beijing Optical Instrument Factory) was used to make differential thermal analysis (DTA) scans in a static air atmosphere. The powdered polymer sample was heated to 237°C at a heating rate of 10°C/min and maintained at this temperature for 5 min to allow

all the crystals to melt. In the cooling cycle, the sample was cooled from 237°C to room temperature under an average cooling rate of 5.63°C/min. The peak temperature of the melting endotherm was defined as the melting point (T_m). The peak and the onset temperatures of the thermal oxidation exotherm were defined as thermal oxidation temperature (T_o) and thermal oxidation onset temperature (T_o'). The peak and the onset temperatures of the crystallization exotherm were defined as the crystallization temperature (T_c) and the crystallization onset temperature (T_c'), respectively. The weight loss ($-W$) was determined by thermogravimetric analysis (TGA).

RESULTS AND DISCUSSION

Morphological Structure

The transmission electronic micrographs of TRPPs samples versus the ratio of EP to SB elastomer and the amount of elastomer in the TMB are shown in Figures 1 and 2, respectively. We observed that the phase morphology exhibited common characteristics of the PP component as a continuous phase and the elastomer component as a dispersed phase with a cellular structure (salami structure). However, differences were observed for different samples. It was clearly observed that TRPPs 4G-I-4 and 4G-II-4 had a structure similar to that of acrylonitrile-BS (ABS) copolymer and high-impact strength polystyrene (HIPS) synthesized by graft copolymerization, in which almost every dispersed domain incorporated with PP formed a cellular structure. However, TRPPs 4G-I-3, 4G-III-4, and 4G-IV-4 had relatively fewer dispersed domains with a cellular structure. The rest of the TRPP samples only had minor dispersed domains with a cellular structure. Moreover, the size of the dispersed phase and its distribution differed greatly. TRPPs 4G-I-4 and 4G-II-4 had relatively smaller, more homogeneous average domain sizes (about 0.48 and 0.42 μm, respectively).

The phase structure difference of the TRPP 4G series was mainly due to the difference in the corresponding TMBs used. TMBs I-4 and II-4, which were used for the preparation of TRPPs 4G-I-4 and 4G-II-4, had a moderate amount of crosslinked elastomer and relatively higher content of PP connected with the elastomers by polymer bridges.[19] Therefore, when phase separation occurs, the dispersed domain size of the elas-

tomers would not be very large for the emulsification of graft and crosslinked copolymers at the interface. Moreover, the PP drawn into the dispersed phase was divided, encapsulated, and finally formed into small coagulations: the cellular structure formation was also attributed to the existence of grafted and crosslinked elastomers and PP at the interface. If the master batch had more crosslinked elastomers and less PP connected with the elastomers by polymer bridges (e.g., TMB I-1), the contraction power of the elastomers dispersed phase would be stronger and the power for PP encapsulation would be weaker during phase separation. This may make it difficult for the dispersed phase to form a typical cellular structure. It was also observed that the cellular structure of TMBs was "transplanted" into the TRPPs upon thermal blending of the TMBs with the PP resin. Simultaneously, it can be expected that the chemical structure would also be transplanted into the corresponding TRPPs.

In a previous article[21] we discussed the dependence of the mechanical properties of TRPPs on the ratio of EP to SB elastomer and the overall elastomer amount in the TMB. It was realized that the TRPPs made from a TMB with an 80/20 (w/w) ratio of EP to SB and overall elastomer amounts of 32 and 38 wt %, respectively (i.e., TRPPs 4G-I-4 and 4G-II-4), appeared to have excellent balanced mechanical properties. For example, the notched Izod impact strength of TRPP 4G-I-4 at 23°C was 762 J/m (which is 23 times that of PP), the flexural modulus was 1078 MPa (92% of PP), and the tensile strength at yield was 34.8 MPa (88% of PP). As found in the present work, TRPPs 4G-I-4 and 4G-II-4 had a typical chemical and morphological structure similar to ABS or HIPS, which produced the high performance of the PP composites. The introduction of the graft and crosslinked copolymer of PP and elastomers on the dispersed particle surfaces improved the affinity between the two phases and also improved the dispersive state of the particles. Moreover, almost all of the dispersed particles incorporated PP into themselves during the polymerization and increased the elastomer apparent volume. On the other hand, the dispersed domain size was small and more elastomer particles functioned as stress concentrators under deformation. At the same time, the elastomer particles promoted crazing or shear yielding in the matrix and suppressed brittle fracture as a result. Hence, it can be easily understood that TRPPs 4G-I-4 and
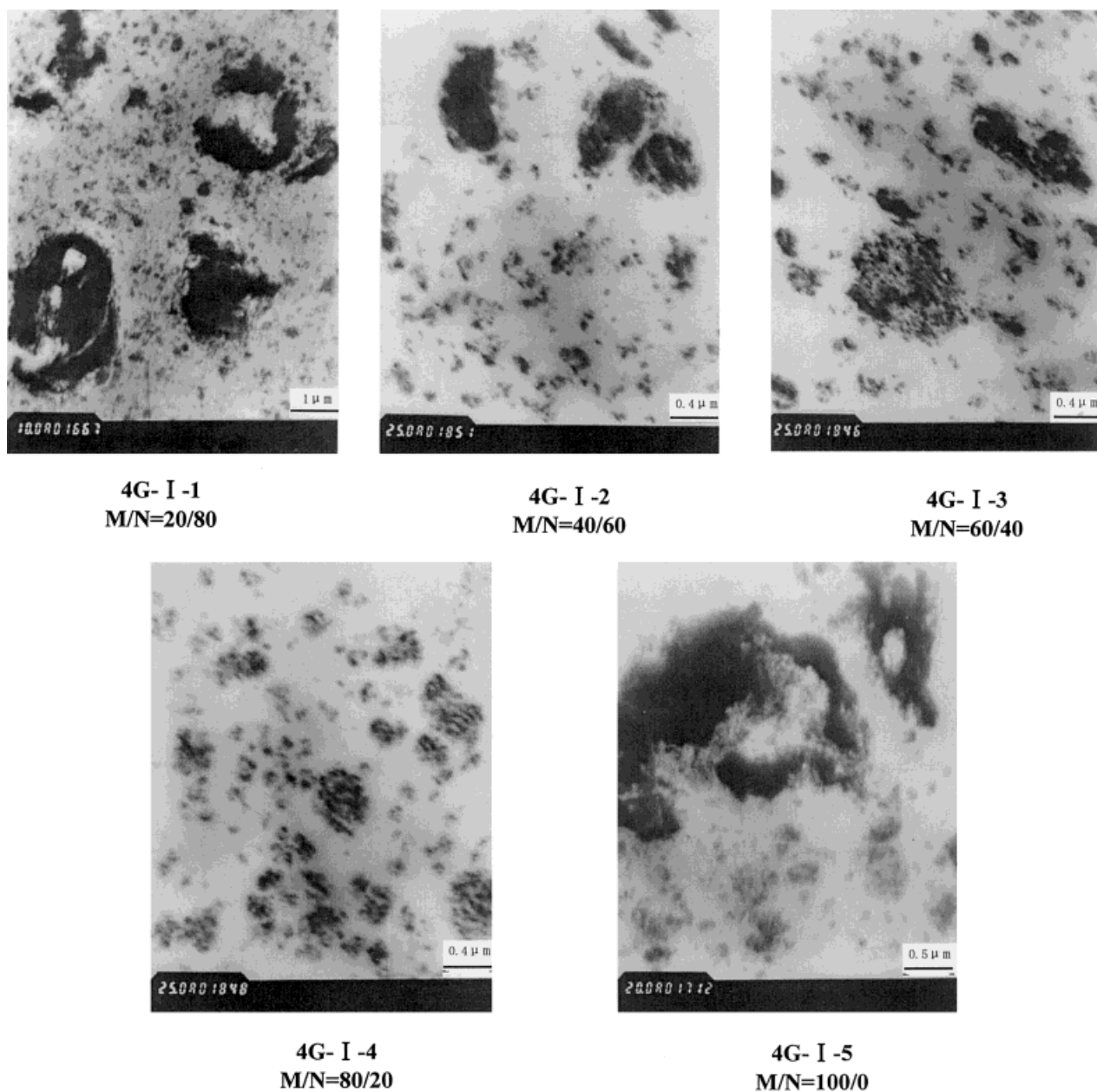
4G- I -1
M/N=20/80

4G- I -2
M/N=40/60

4G- I -3
M/N=60/40

4G- I -4
M/N=80/20

4G- I -5
M/N=100/0

Figure 1 Transmission electron microscopy photographs of TRPPs with different ratios of the EP (M) and SB (N) elastomers.

4G-II-4 should have better mechanical properties than the rest of the TRPPs.

Figures 3–5 show the polarizing micrographs of TRPPs with various compositions, pure PP, and a sample 0G-0i simply blended with PP. It can be seen that under the same crystallization conditions, the crystal structure of pure PP was more perfect, the spherulite size was larger, and the spherulitic boundaries were clear. The PP in a comparative sample 0G-0i also formed spherulites with a little

smaller size than that of pure PP because of the nucleation of the elastomers.[22] It was also observed that there were some elastomer particles dispersed on the spherulites. However, the crystallite size of the PP in the TRPPs was remarkably reduced. There were slight differences among samples with different compositions. For example, the crystallite size of the PP in TRPPs 4G-I-4, 4G-II-4, 4G-III-4, and 4G-IV-4 was increased in turn. In addition, the crystallite size of the PP in TRPP 4G-I-5, in which
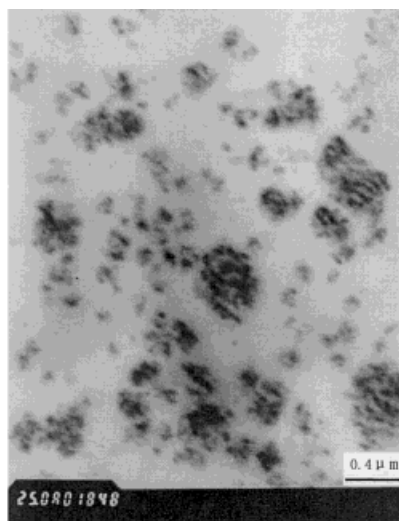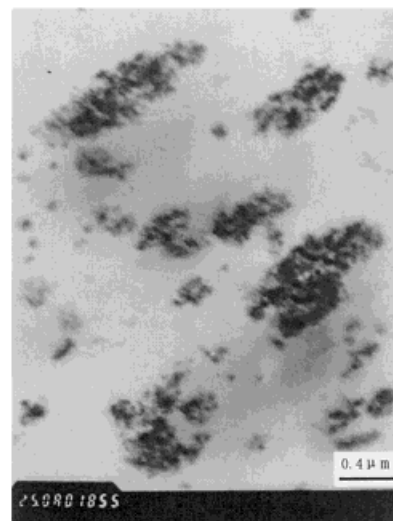
4G-I-4
M+N in TMB: 32wt%
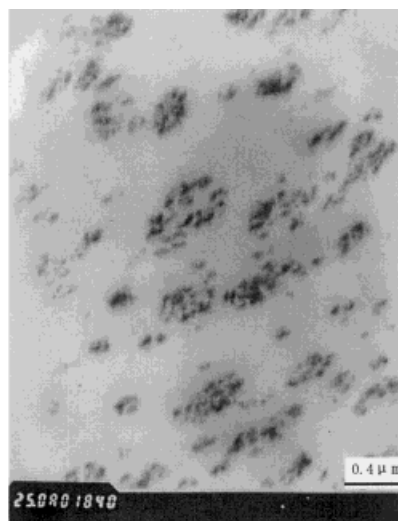
4G-II-4
M+N in TMB: 38wt%
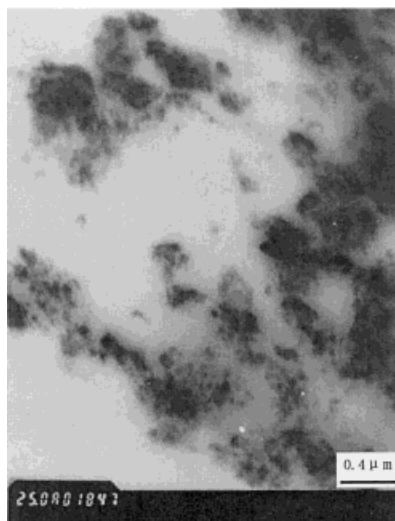
4G-III-4
M+N in TMB: 44wt%

4G-IV-4
M+N in TMB: 50wt%

Figure 2 Transmission electron microscopy photographs of TRPPs with different EP (M) and SB (N) elastomer amounts in the TMB.

only EP elastomer was present, was larger than that of all the other TRPPs.

As we reported earlier,[20] the crystalline morphology of the PP in TMBs is mainly affected by nucleation of the elastomers and graft copolymer and by the decreased mobility of the PP segments that is induced by the conjunction of PP with the elastomers through a polymer bridge. These effects are much stronger in the TRPPs than in the comparative sample 0G-0i. Therefore, the crystallite size of the PP in TRPPs is substantially reduced compared to 0G-0i. Nevertheless, in the TRPPs with different compositions, the above two effects were not equivalent for the slight difference in chemical structure,[19] thereby leading to the different degrees of reduction in the crystallite size.

Crystallization Behavior

Crystallization exotherms were observed during the cooling cycle of the DTA scans in the temper-
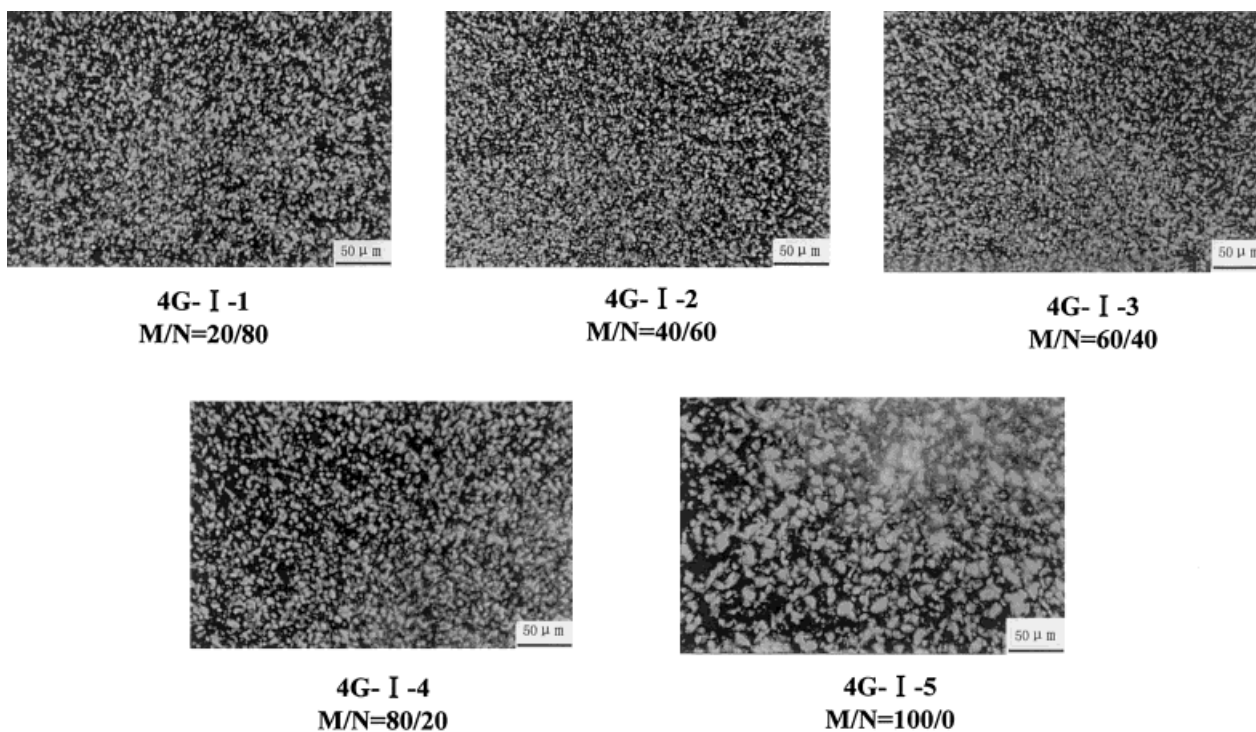
Figure 3 Polarizing light microscopy photographs of the crystalline morphology for TRPPs with different ratios of the EP (M) and SB (N) elastomers.
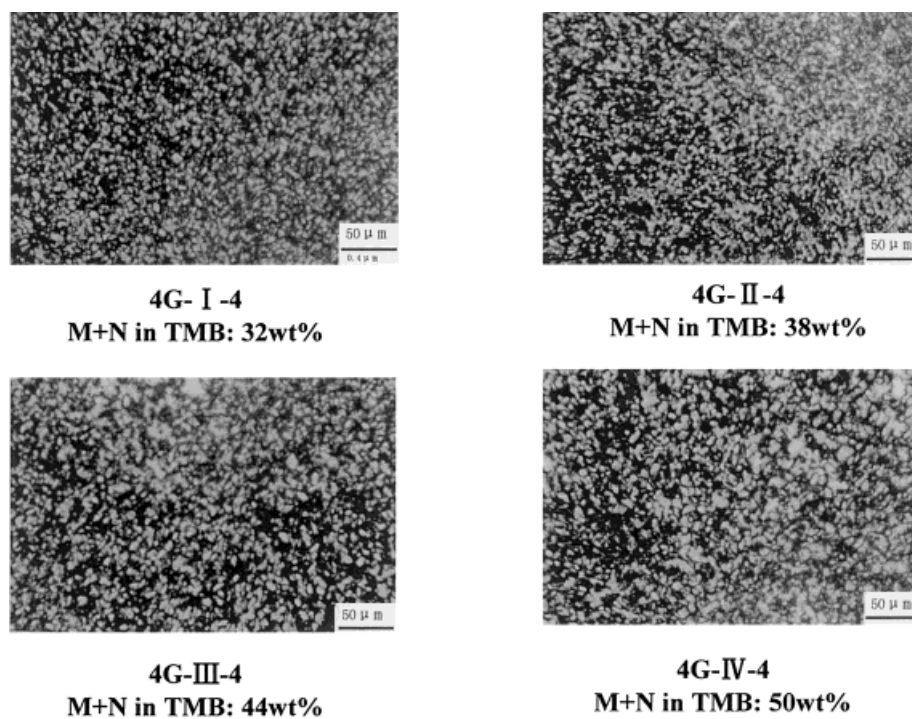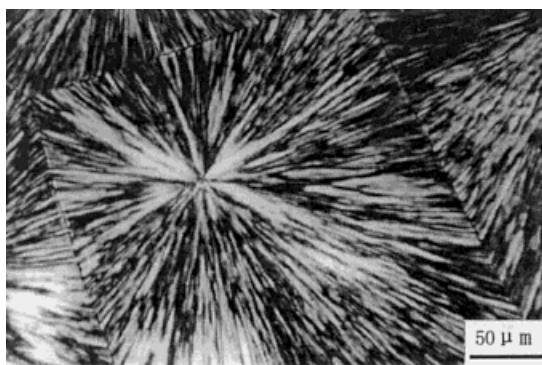

Figure 4 Polarizing light microscopy photographs of the crystalline morphology for TRPPs with different EP (M) and SB (N) elastomer amounts in the TMB.

Simply blended sample 0G-0i

Figure 5 Polarizing light microscopy photographs of the crystalline morphology for PP and the simply blended sample 0G-0i.

ature range of 128–100°C (Fig. 6). Crystallization exotherms were characterized by determining the T_c and T_c' (Table II). A slight increase in the T_c and T_c' was found in pure PP, the simply blended sample 0G-0I, and TRPP. The crystallization of PP was mainly affected by the nucleation of the grafting copolymer in the TRPPs and by the enhanced cohesion between the PP and elastomers for the existence of the polymer bridge. The former caused PP to crystallize at higher temperatures and the latter made it difficult for the PP molecule to align in the crystal lattice, leading to the crystallization at a lower temperature. The above results indicated that the former factor was dominant. It should be noted that TRPP 4G-I-4 had the smallest T_c, which may be attributed to its typical cellular structure.

Thermal Properties

Melting and oxidation endotherms were also observed during the heating cycle of the DTA scans

in the temperature range of 160–240°C (Fig. 6). The endotherms were characterized by the T_m, the T_o, and the T_o'. The $-W$ of the samples was calculated from the TGA data (Table II).

The TRPPs had a little lower T_m than PP and almost the same value as the comparative sample 0G-0i. Moreover, there was only a slight difference between the different samples, indicating that the T_m does not depend on the composition.[23] The observed decrease in the T_m values can be interpreted as being a result of differences in dimension and structure of PP crystallites with pure PP, along with the effects of the strong mobility of the elastomer segments.

The T_o' and T_o of the TRPPs were decreased in varying degrees compared with PP. The decreases were related to the ratio between the two elastomers. For example, from TRPP 4G-I-1 to 4G-I-5, the T_o' and T_o were both reduced with an increase of EP elastomer content. In 4G-I-5, only EP elastomer was used; the T_o' and T_o were almost the same with PP. These results indicated that the decrease in T_o' and T_o was a consequence of the presence of double bonds in the SB elastomer.

Most of the TRPPs had a lower $-W$ value than PP, but some were higher. From the molding process of standard specimens it was observed that the TRPPs had a processability similar to PP.
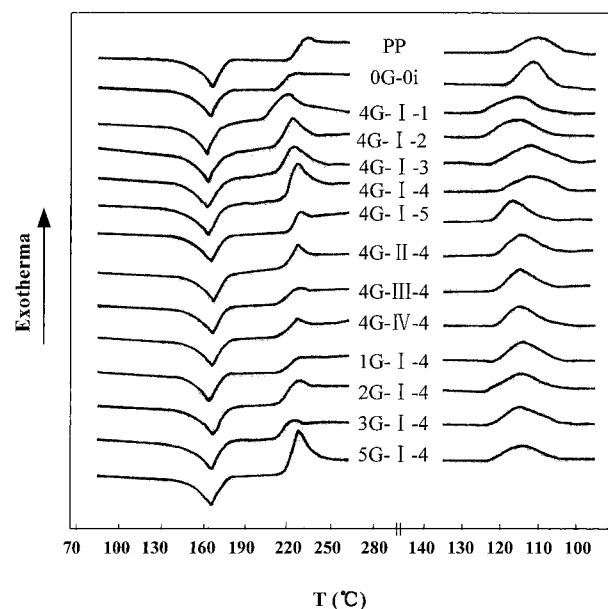

Figure 6 DTA curves of PP, simply blended sample 0G-0i, and TRPPs with different compositions.

Table II   Thermal Analysis Data of PP, 0G-0i, and TRPPs

Entry	T_c' (°C)	T_c (°C)	T_m (°C)	T_o' (°C)	T_o (°C)	$-W$ (%)
PP	120.4	110.6	166.5	220.0	231.1	2.67
0G-0i	119.7	111.9	164.8	210.4	226.6	2.47
4G-I-1	127.5	114.5	163.0	199.0	223.9	1.72
4G-I-2	126.2	114.5	163.6	205.0	224.4	2.2
4G-I-3	124.3	112.6	163.3	209.2	226.0	2.09
4G-I-4	121.5	111.9	163.0	212.8	227.7	2.76
4G-I-5	123.0	117.1	164.8	217.6	229.9	3.17
1G-I-4	122.1	113.8	163.6	214.6	229.9	3.07
2G-I-4	122.3	114.5	164.8	212.8	226.6	3.24
3G-I-4	122.3	115.1	164.8	212.8	227.1	2.71
4G-I-4	121.5	111.9	163.0	212.8	227.7	2.76
5G-I-4	122.3	114.5	164.8	212.8	228.2	3.08
4G-I-4	121.5	111.9	163.0	212.8	227.7	2.76
4G-II-4	122.3	114.5	165.4	215.2	226.6	2.22
4G-III-4	122.3	114.5	164.8	213.4	226.6	2.46
4G-IV-4	122.0	114.5	164.8	212.8	228.2	1.88

CONCLUSIONS

The TRPPs prepared by thermal mechanical blending of PP resin with TMBs had a morphological character with the PP component as the continuous phase and the elastomer component as the dispersed phase with a cellular structure (salami structure) containing some PP. The particles of the dispersed phase were small and regular. The cellular structure of TRPPs resulted from the introduction of TMBs and it was similar to ABS and HIPS. During gradual cooling from the melt, the crystallization of TRPP was nucleated heterogeneously and the crystallization temperature was slightly higher than that of PP whereas the crystal size was substantially reduced. The T_m, T_o, and T_o' were all slightly lower than those for pure PP.

REFERENCES

1. Jiang, W.; Liu, C. H.; Wang, Z. G. Polymer 1998, 39, 3285.
2. Saroop, M.; Mathur, G. N. J Appl Polym Sci 1997, 65, 2691.
3. Kim, Y. K.; Cho, W. J.; Ha, C. S. Polym Eng Sci 1995, 35, 1592.
4. Inoue, T. J Appl Polym Sci 1994, 54, 723.
5. Inoue, T.; Suzuki, T. J Appl Polym Sci 1995, 56, 1113.
6. Stehling, F. C.; Huff, T.; Speed, C. S.; Wissler, G. J Appl Polym Sci 1981, 26, 2693.
7. Jancar, J.; Di Anselmo, A.; Di Benedetto, A. T.; Kucera, J. Polymer 1993, 34, 1684.
8. Favis, B. D. J Appl Polym Sci 1990, 39, 285.
9. George, S.; Joseph, R.; Thomas, S.; Varughese, K. T. Polymer 1995, 36, 4405.
10. Stricker, F.; Thomann, Y.; Mulhaupt, R. J Appl Polym Sci 1998, 68, 1891.
11. Kolarik, J.; Jancar, J. Polymer 1992, 33, 4961.
12. Bartczak, Z.; Argon, A. S.; Cohen, R. E.; Weinberg, M. Polymer 1999, 40, 2331.
13. Wong, S. C.; Mai, Y. W. Polymer 1999, 40, 1553.
14. Zhang, Z.; Chiu, D. S.; Siu, G. J Reinf Plast Compos 1997, 16, 603.
15. Zhang, Z.; Chiu, D. S.; Siu, G. J Reinf Plast Compos 1996, 15, 452.
16. Zhang, Z.; Chiu, D. S.; Siu, G. J Reinf Plast Compos 1996, 15, 74.
17. Petrovic, O. S.; Bullings, J.; Simendic, K. J Appl Polym Sci 1996, 59, 301.
18. D'Orazio, L.; Mancarella, D.; Martuscelli, E.; Cecchin, C.; Corrieri, R. Polymer 1999, 40, 2745.
19. Zhang, H. J.; Wang, J. W.; Cao, S. K.; Shan, A. G. Polym Adv Technol 2000, 11, 334.
20. Zhang, H. J.; Wang, J. W.; Chen, M. J.; Cao, S. K.; Wang, X. Q. Polym Adv Technol 2000, 11, 342.
21. Zhang, H. J.; Wang, J. W.; Li, J.; Cao, S. K.; Shan, A. G. J Appl Polym Sci 2001, 79, 1345.
22. Wu, P. X.; Zhang, L. C. Polymer Blends and Modification; Chinese Light Industry Press: Beijing, 1996.
23. Martuscelli, E.; Silvestre, C.; Abate, G. Polymer 1982, 23, 229.